Chapter 10
Neuropathology of Mild Traumatic Brain Injury: Relationship to Structural Neuroimaging Findings

Erin D. Bigler

Abstract The basics of structural neuroimaging identified neuropathological changes that may be identified on computed tomography and magnetic resonance imaging associated with mild traumatic brain injury (mTBI) are reviewed. Emphasis is placed on understanding the subtle nature of neuropathology that may accompany mTBI and its detection with neuroimaging. The role of diffusion tensor imaging is overviewed with numerous examples provided that illustrates neuroimaging techniques that detect mTBI abnormalities.

Keywords Mild traumatic brain injury (mTBI) concussion • Neuropsychology neuroimaging • Biomarkers • Neuropathology brain damage cognitive and neurobehavioral sequelae

Introduction

The limits of neuroimaging specify what types of neuropathology can be detected in traumatic brain injury (TBI), especially if the injury is mild. Fortunately, tremendous advances in neuroimaging technologies especially with magnetic resonance imaging (MRI) have been made over the last decade, even in detection of subtle pathology following mild traumatic brain injury (mTBI). Most conventional MRI studies configure anatomical images with millimeter resolution, meaning MRI detects pathology at a similar level of resolution, although submillimeter resolution

E.D. Bigler, Ph.D. (✉)
Department of Psychology and Neuroscience Center, Brigham Young University, 1190D Kimball Tower, Provo, UT 84602, USA

Department of Psychiatry, University of Utah, Salt Lake City, UT, USA
e-mail: erin_bigler@byu.edu

S.M. Slobounov and W.J. Sebastianelli (eds.), *Concussions in Athletics: From Brain to Behavior*, DOI 10.1007/978-1-4939-0295-8_10,

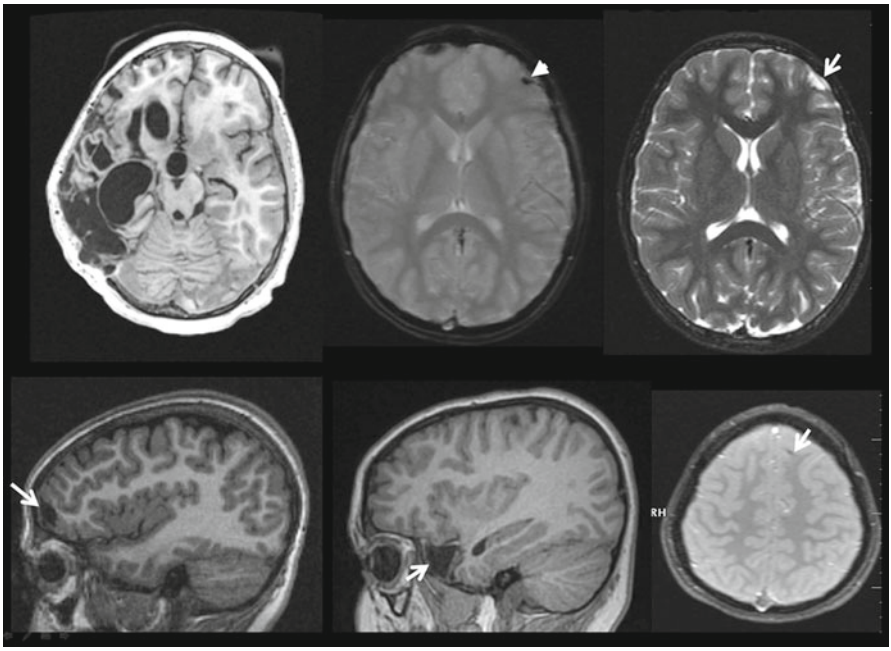

Fig. 10.1 The subtleness and diversity of MRI identified chronic (>6 months post-injury) brain lesions in four mTBI patients, all with a GCS of 15, compared to the massive structural pathologies associated with severe TBI are presented in this figure. The mTBI case shown in the *top middle* and *right* shows characteristic area of small focal encephalomalacia with increased region of CSF (*arrow*) in the T2-weighted image (*top right*) associated with residual hemosiderin (*arrowhead*) in the gradient-recalled echo (GRE) sequence (*top middle*). These pathological changes were originally the result of a focal frontal contusion. In the sagittal image in the *bottom left*, focal frontal encephalomalacia is evident (*arrow*) and encephalomalacia in the temporal lobe (*arrow*) in the *middle* image with the *bottom right* image showing an axial scan with subtle hemosiderin right at the gray-white junction (*arrow*). In contrast, the child with severe injury (axial view, *upper left*) has massive structural pathology. From Bigler ED, Abildskov TJ, Petrie J, Dennis M, Simic N, Taylor HG, et al. Heterogeneity of brain lesions in pediatric traumatic brain injury. *Neuropsychology*. 27(4), 438-451, 2013; used with permission

is now possible [1, 2]. However, the fundamental pathological changes that occur from TBI happen at the micron and nanometer cellular level [3, 4]. This means for brain injuries in the mild range, with the subtlest of neural injury that the macroscopic lesions characteristic of more severe injury are simply not visible in most cases. Straightforwardly, the contrast in gross visible detection of pathology from mild to severe TBI is demonstrated in Fig. 10.1.

In Fig. 10.1 all of the individuals with mTBI had a post-resuscitation Glasgow Coma Scale [5] score of 15 and were part of the Social Outcomes of Brain Injury in Kids (SOBIK [6]) investigation. Although all children in the SOBIK investigation who sustained mTBI had positive day-of-injury (DOI) computed tomography (CT), only about two-thirds of the 41 mTBI children had identifiable abnormalities when

followed up approximately a year or more post-injury. As demonstrated in the Bigler et al. [6] investigation a number of the children with subtle hemorrhage and/or localized edema on the DOI CT did not evidence visibly detectable abnormalities on follow-up MRI performed at least a year post-injury. While not possible in human mTBI studies, animal investigations that model mTBI where acute neuroimaging abnormalities become non-detectable over time nonetheless may show histological pathology [7, 8]. As such, it is safe to assume that DOI pathology like petechial hemorrhages that are not detected on follow-up imaging nonetheless indicate significant shear forces were present in the brain at the time of injury and likely do reflect where residual pathology may be present at the cellular level, just not detectable with contemporary neuroimaging methods.

Because of these limitations with neuroimaging resolution in detecting abnormalities, a simple dichotomy in structural imaging may be developed between lesions or abnormalities visibly identified at the macroscopic level and those more empirically or quantitatively derived from scan metrics. This distinction between visible versus empirically derived quantitative metrics will be further explored in this chapter but first some mention of the role of CT in TBI will be discussed because it is the most common initial or emergently performed imaging modality performed in TBI, including mTBI [9, 10]. As such, typically the first neuroimaging findings in TBI are CT based, providing important baseline information even when entirely negative. This chapter will not cover functional neuroimaging or magnetic resonance (MR) spectroscopy (MRS) as these techniques will be covered elsewhere and have previously been reviewed by Slobounov et al. [11]. Also, fundamentals of imaging will not be covered in this chapter as a variety of publications provide such information [12–14].

Heterogeneity of MTBI

As already alluded to in Fig. 10.1, no two head injuries are identical [15]. Even with the careful precision of animal models no two injuries can ever be identically replicated [16]. If one now adds to the complexity individual differences in human development and experience (the brain is an experience/age-dependent organ), combined with genetic endowment and whatever unique circumstances that occur with each injury, an incredible mix of events and circumstance accompanies every injury. So the pathology that is detectable via neuroimaging techniques will never be identical across individuals but there are common pathologies. As will be explained in greater detail throughout this chapter, particular vulnerability of white matter (WM) underlies much of the pathology associated with mTBI. Many axons are myelinated; with the vulnerability of WM damage from trauma the WM designation infers that the axon element of the neuron is particularly vulnerable in TBI. Interneuronal connection occurs via axons; thus, WM pathology in TBI may be considered a problem of neural connectivity. With a neuron's cell body densely compacted within the neuropil

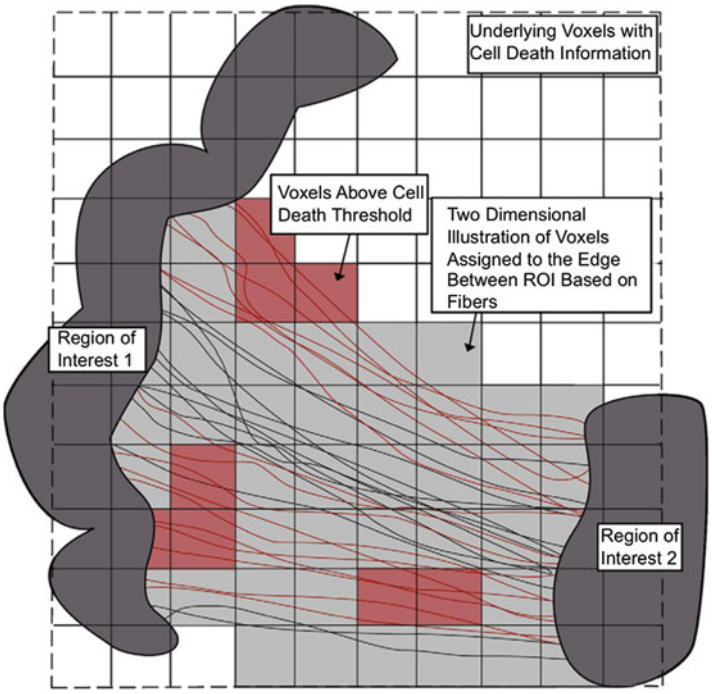

Fig. 10.2 This schematic shows how different axon trajectories may or may not be vulnerable to injury. As can be seen, there are only certain sectors where the biomechanical deformation sufficiently alters brain parenchyma to damage axons. *Lines* represent hypothetical axon projections from one gray matter structure to another. Note that even though all connect region of interest (ROI) 1 with ROI 2, and that out of all sectors where these hypothetical axons project, only eight of the sectors experienced sufficient deformation to damage axons, because of the differences in crossing routes and trajectories numerous axons were affected. From Kraft RH, McKee PJ, Dagro AM, Grafton ST. Combining the finite element method with structural connectome-based analysis for modeling neurotrauma: connectome neurotrauma mechanics. (*PLoS Comput Biol*. 2012; 8(8): e1002619; used with permission

of the gray matter and held tightly within this matrix of cell bodies, the axon extension becomes vulnerable because WM pathways course in multiple directions of various lengths creating a bend and interwoven lattice work of projecting axons making WM especially vulnerable to stretch, strain, and tensile effects following the mechanical deformation that occurs with impact injury [17, 18]. This is depicted in Fig. 10.2 which shows that only certain WM tracts are actually damaged within a particular biomechanical strain field (see [19]). Watanabe et al. [20] have shown how with each individual impact injury, unique influences occur from the biomechanical movement of the brain within the cranium. These unique individual differences, when coupled with the fact that neural tissue has different elastic properties that are region and structure dependent [21, 22], demonstrate that no two injuries from mTBI will ever produce identical pathology detectable by neuroimaging.

Time Sequence of Neuropathology Associated with MTBI

There can be no dispute that an acute brain injury has occurred in a witnessed traumatic event associated with positive loss of consciousness (LOC) and obvious biomechanical forces. Therefore, such cases represent the best model for understanding the time sequence of symptom resolution and return to baseline function. The case shown in Fig. 10.3, which displays a negative DOI CT scan, provides such an example. This young adult female sustained an mTBI in an auto-pedestrian accident.

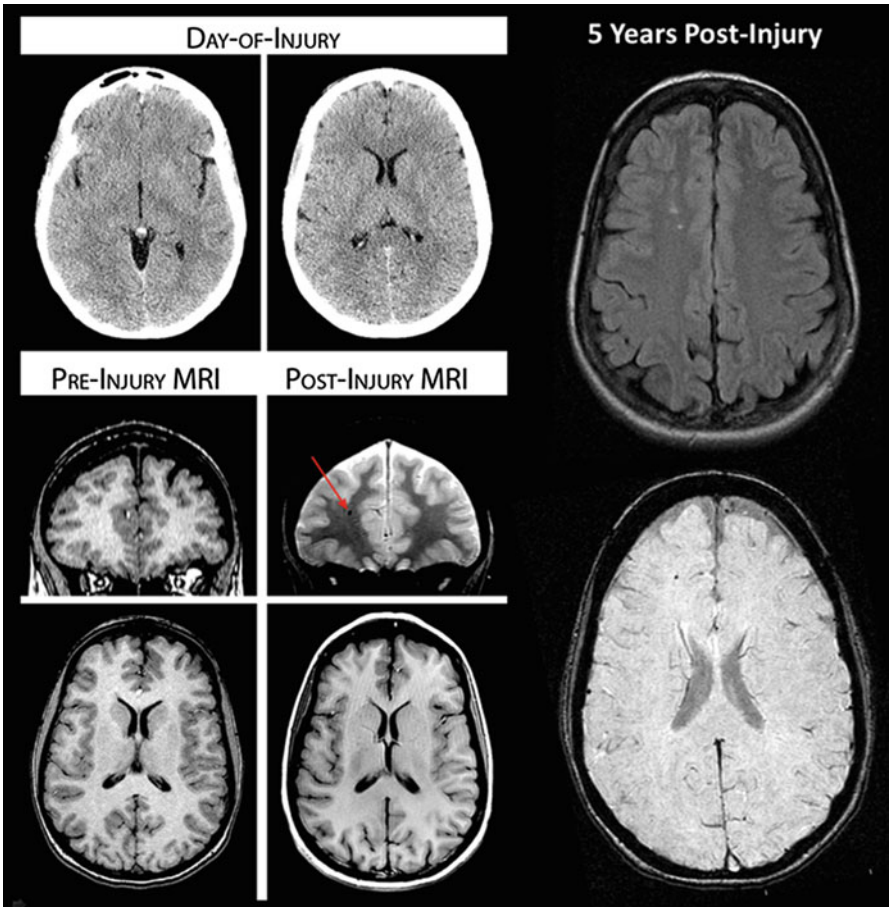

Fig. 10.3 This young adult sustained a significant mTBI in an auto-pedestrian injury where she had positive LOC, but the DOI CT revealed no abnormality. However, as symptoms persisted this patient was assessed with MRI which revealed hemosiderin and focal white matter hyperintensities. Interestingly, this patient had participated as a research subject prior to the injury, confirming no prior brain abnormalities, as shown in the pre-injury MRI, although only a T1-weighted MRI had been performed (courtesy of Geri Hanten, Ph.D.)

She was struck by a passing car while standing next to her vehicle with family members nearby, but no other family member was struck or injured. She was thrown into the air striking her head on the curb, resulting in immediate LOC (no skull fracture), which lasted 2–3 min according to eyewitness family members present at the time of the accident. Emergency medical services were on the scene within 10 min, where they found her conscious but confused. She had orthopedic injuries to her legs (ligament knee injuries), was stabilized and transported to the emergency department (ED) with a GCS of 15 noted on intake. During ED observation over the next couple of hours, GCS fluctuated between 13 and 15. With the head CT being negative (see Fig. 10.3), but given the severity of the impact, positive LOC and fluctuating level of GCS she was monitored overnight and discharged the next day, with outpatient follow-up provided through the hospital concussion care program. Interestingly, her post-concussive symptoms (PCS) of headache, mental confusion, lethargy, and sleepiness increased in the days that followed. Some have speculated that PCS reaches its apex on the DOI and then dissipates. While true for some, peak symptoms following mTBI may occur hours to days post-injury [23, 24], which was the case with this patient. She was a student and attempted to go back to her studies approximately 3 weeks post-injury but experienced major cognitive challenges, especially in terms of problems with focused and sustained attention. Because of the persistence in symptoms and that MRI studies had not been done, an MRI was obtained which demonstrated residual hemosiderin deposition scattered in the right frontal region as shown in Fig. 10.3, that also corresponded with scattered WM hyperintensities. These abnormalities remained stable over the next 5 years and represent common neuroimaging sequelae associated with mTBI. The follow-up scans objectively document the damage from the mTBI and also demonstrate the insensitivity of CT in detecting some micro-hemorrhages associated with mild injury as well as other pathologies that undoubtedly, given the MRI findings, were present on the DOI but below the threshold for CT detection. With regard to the timeline of symptom onset, what is of particular interest as demonstrated in this case is that it took several days for the full effects of the mTBI to be manifested and weeks to diminish but chronic deficits remained as would be expected given the MRI findings, consistent with shear damage within the frontal lobes.

Although the positive LOC in mTBI is abrupt and an obvious indicator of TBI, by definition for mTBI it has to be brief and transient or otherwise, the injury would no longer be considered “mild.” The evolution of symptoms/problems associated with the initial injury likely has much to do with complex cellular responses to the mechanical deformation of brain parenchyma following injury which is overviewed in Fig. 10.4. [25]. Review of Fig. 10.4 clearly indicates that while mTBI is initiated by an event involving traumatic deformation of neural tissue, the event does not induce a singular pathological event, but initiates the most complex array of structural and physiological changes in brain parenchyma. If the biomechanical deformation is minimal, only transient disruption in neuron integrity occurs [26]. This is depicted in Fig. 10.5 [27], based on cultured neurons, that have been mechanically stretched to mimic injury, from minimal and transient to maximal with permanent damage. This illustration provides a nice heuristic, albeit simplistic, to visualize

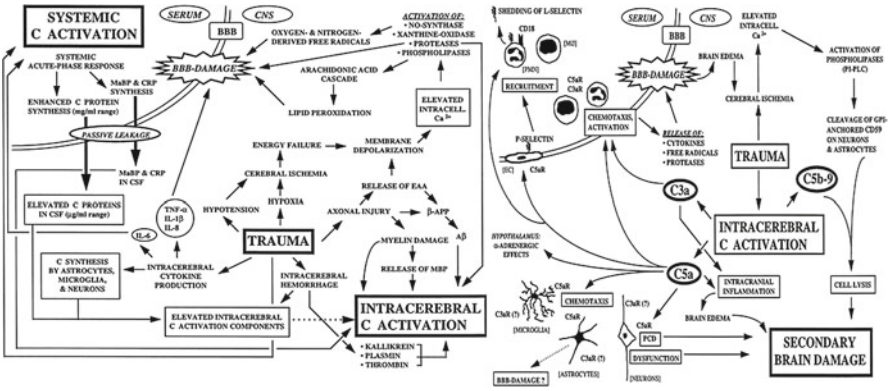

Fig. 10.4 These illustrations depict the primary (A-*left*) and secondary (B-*right*) mechanisms of pathology that occur from TBI. (A-*left schematic*) Cascade of pathophysiological events following traumatic brain injury: mechanisms of elevated complement levels and complement activation within the injured brain (the "C" abbreviation stands for the complement system, an important effector arm of the immune system in the defense against invading pathogens; see Stahel et al. [25] for details and additional explanations of the abbreviations and explanations about their interactions). (B-*right schematic*) Potential mechanisms of complement-mediated secondary brain damage following intrathecal complement activation in head trauma. *EC* endothelial cells, *MØ* monocytes/macrophages, *PMN* polymorphonuclear leukocytes; *?*, cell type-specific function unknown at present; again see Stahel et al. [25] for other abbreviations and explanations. From Stahel PF, Morganti-Kossmann MC, Kossmann T. The role of the complement system in traumatic brain injury—review. *Brain Res Brain Res Rev*. 1998; 27(3): 243–256; used with permission

what may occur following mTBI. Note in this heuristic, transient injury may not lead to structural damage. In such a scenario, the injury did not reach a severity threshold where reparative influences could not overcome the initial cascade of potentially permanent damaging effects from the traumatic pathophysiological events. However, with more significant perturbation, the deformation may begin a process that results in irregular axon morphology and synaptic discontinuities to complete axonal degradation.

Even the briefest viewing of Figs. 10.4 and 10.5 demonstrates the complexity of what attends even a mild injury but the timing of when pathology is expressed further complicates what may be detected with neuroimaging techniques. For example, Morrison et al. [28] show the complexity of the pathobiology of TBI based on severity and time post-injury in an in vitro model of stretch injury as depicted in Fig. 10.6. In this model immature hippocampi are removed, cultured, and then subjected to stretch injury. Dependent on the severity of stretch and time post-injury reflects differences in damage, some damage may be immediately sufficient to cause cell death whereas other cells may just be rendered physiologically instable but with the potential to return to baseline whereas others die.

However, if an injury is to be but a transient perturbation of physiological integrity, a large array of cellular functions, as depicted in Fig. 10.4, must overtime return

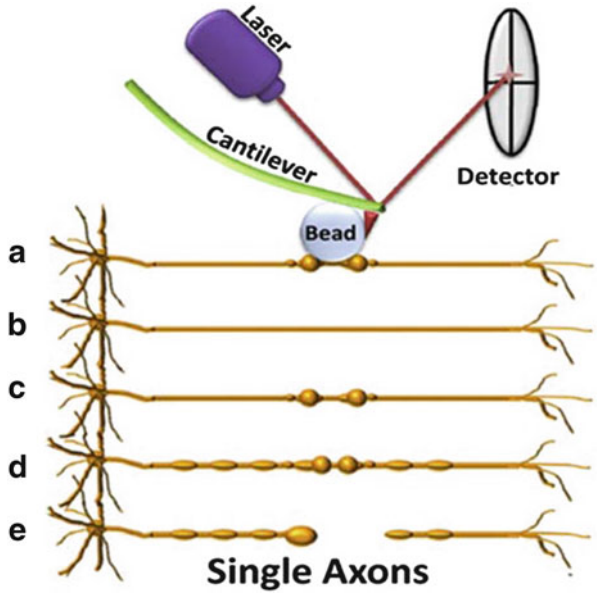

Fig. 10.5 This illustration depicts various potential axonal outcomes following stretch injury in an in vitro TBI model. (**a**) Shows stretch sufficient to create axon beading, which may have transient effect if minimal enough and as shown in (**b**) where axon morphology returns to baseline with no identifiable structural abnormality. However, initial beading may progress, as shown in (**c**) and (**d**), resulting in axon discontinuity and degeneration as shown in (**e**). From Magdesian MH, Sanchez FS, Lopez M, Thostrup P, Durisic N, Belkaid W, et al. Atomic force microscopy reveals important differences in axonal resistance to injury. *Biophys J*. 2012; 103(3): 405–414; used with permission

to homeostatic baseline. Translating this into what may occur in human mTBI, Fig. 10.7 shows how cognitive and neuroimaging findings change over time in mTBI during the first 8 days [29]. All of these mTBI patients had experienced an "uncomplicated" mTBI meaning that no abnormalities were identified in the DOI CT scan, almost all with a GCS of 15 and all the result of some type of motor vehicle accident. All subjects were assessed within 2 days of injury, and serially at days 3–4, 5–6, and 7–8 post-injury. Alternate forms of the Hopkins Verbal Learning Test-Recall (HVLT-R) were administered at each time point and as can be seen in Fig. 10.7, memory performance typically dipped between days 3–6, suggesting the confluence of primary and secondary effects from mTBI reaching their apex at this point. Interestingly, these subjects were also assessed at each time point with MRI and diffusion tensor imaging (DTI), where the fractional anisotropy (FA) measurement was obtained on each occasion. As plotted in Fig. 10.7, FA exhibited variable fluctuations within each individual as did memory function over the first 8 days post-injury. In mTBI acute increases in FA may reflect neuroinflammation [30] and as seen in Fig. 10.7, several mTBI patients showed FA peaks between days 3–4 and 7–8. Decrease in FA may reflect axon damage and without pre-injury neuroimaging

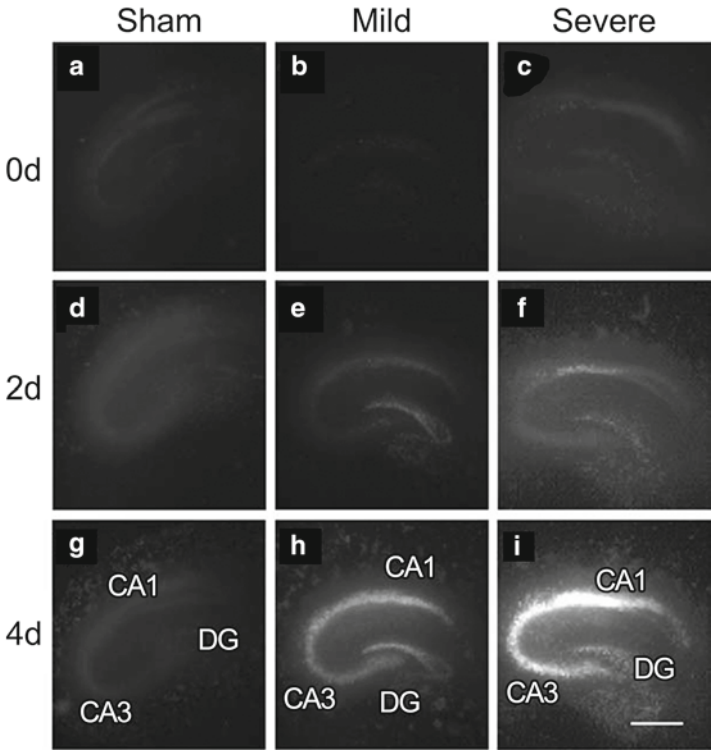

Fig. 10.6 The severity and timing of pathological changes is critical in understanding the effects of TBI. This in vitro cultured hippocampal study shows that neuronal pathology from injury takes days to be expressed and is proportional to severity of injury (mild, moderate, and severe stretch injury). *0d* represents the time point immediately after injury, *2d* represents the second-day post-injury and *4d* indicates the fourth-day post-injury. The images on day 0 show no distinct fluorescence and but a fuzzy appearance by the second day. However, by the fourth day extensive changes had occurred, distinctly more prominent in the severe injury sample. These investigators used propidium iodide fluorescence to microscopically detect cell damage where only damaged cells fluoresce with the degree of fluorescence reflective of the amount of damage. Clearly evident is that it took 4 days for cell damage to be prominently expressed, but even in the mild stretch condition cellular pathology occurred. Such findings support the development of symptoms associated with mTBI to take hours to days to reach an apex (scale bar = 1 mm). From Morrison B, Cater HL, Benham CD, Sundstrom LE. An in vitro model of traumatic brain injury utilising two-dimensional stretch of organotypic hippocampal slice cultures. *J Neurosci Methods*. 2006;150(2): 192–201; used with permission

to know precisely where each individual's FA baseline made it difficult to fully interpret these findings. However, from a memory performance perspective, almost all showed a decrease after day 1–2, with PCS symptoms reaching their peak around day 3. This does suggest that the variability in FA during this acute/subacute time frame may reflect instability of WM microstructure associated with the injury.

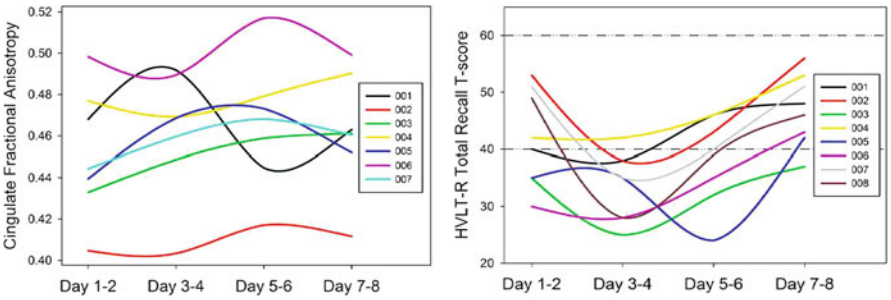

Fig. 10.7 Fractional anisotropy (FA) serial plots over the first 8 days post-injury for seven mTBI patients plotted with corresponding memory performance on the Hopkins Verbal Learning Test-Recall (HVLT-R) performed on the same day as the neuroimaging (note one patient did not have the serial neuroimaging performed). Note the fluctuation in FA, but also the general reduction in memory performance between days 3–4 and 7–8. From Wilde EA, McCauley SR, Barnes A, Wu TC, Chu Z, Hunter JV, et al. Serial measurement of memory and diffusion tensor imaging changes within the first week following uncomplicated mild traumatic brain injury. *Brain Imaging Behav*. 2012; 6(2): 319–328; used with permission

Computed Tomography in MTBI

CT imaging is especially rapid and with contemporary technology can be completed within seconds to minutes in the acutely injured individual. Since it uses X-ray beam technology, it is not influenced by paramagnetic objects like MRI and therefore life-support and other medical assist devices do not interfere with image acquisition or preclude the use of MRI. Likewise, metallic fragments from injury that may be paramagnetic can be imaged without concern about displacement by the strong magnetic fields generated by MRI. Excellent contrast between bone and brain parenchyma can be achieved with CT, where CT clearly has the advantage over MRI in demonstrating the presence and location of skull fractures, common sequelae with head injury. CT also provides methods for examining cerebrovasculature and inflammation in TBI.

In mTBI the commonly identified abnormalities are surface contusions typically at the brain–skull interface, petechial hemorrhages, and/or localized edema. The presence of petechial hemorrhage in TBI is considered a marker of DAI [31, 32], two examples of which are shown in Fig. 10.8. Skull fracture is also readily identifiable with CT and must be considered as an indicator of potential brain injury because the distinct forces necessary to fracture bone are certainly sufficient to injury brain parenchyma. Often because of the limited resolution of CT, even in the presence of some type of skull fracture in an individual with mTBI, parenchyma may appear normal on CT. Of course, just because neural tissue may appear "normal" does not mean normal microstructure and function because that is beyond the scope of what CT may detect.

When an abnormality is present on the DOI CT, as stated earlier, often the classification of "complicated mild TBI" is made. However, given contemporary advances

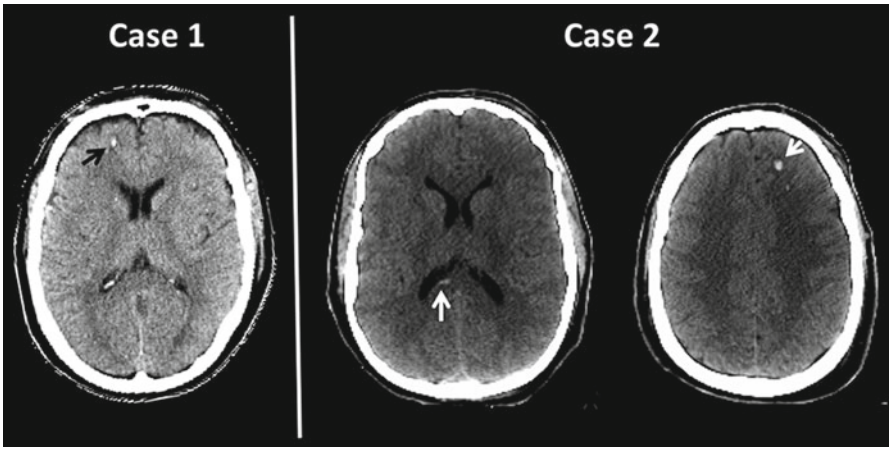

Fig. 10.8 CT appearance of petechial hemorrhage in two separate cases. Note the proximity of the lesion within the white matter but at the border of where the gray boundary is located. Both cases were adults and involved high-speed motor vehicle accidents. Note the *black arrow* in *Case 1* and the *top white arrow* in *Case 2* point to the hemorrhage which occurs right at the gray-white junction. In *Case 2* there is a contrecoup hemorrhagic lesion in the posterior corpus callosum, *bottom arrow*

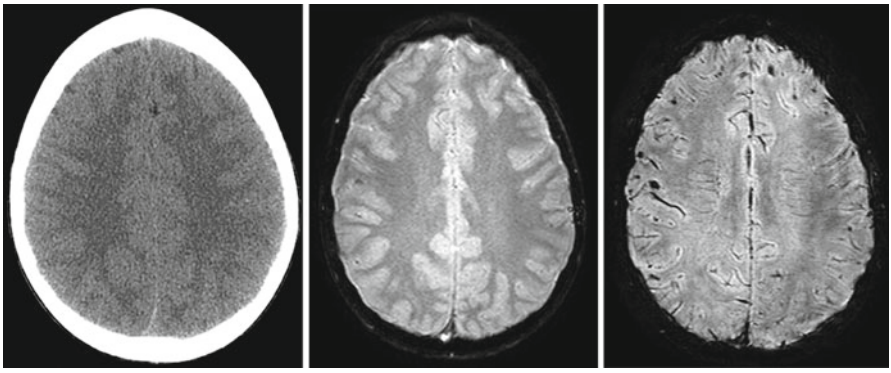

Fig. 10.9 The insensitivity of CT (A) and conventional gradient recalled echo (GRE, B) sequences to detect petechial hemorrhage is shown. The CT scan was interpreted to be within normal limits with no hemorrhage identified yet this individual agreed to participate in a research study and therefore was scanned with MRI procedures including susceptibility weighted imaging (SWI) as shown in (C) and magnetization transfer imaging (MTI, not shown) both show frontal abnormality and residual hemorrhage. From Bigler ED. Neuropsychology and clinical neuroscience of persistent post-concussive syndrome. *J Int Neuropsychol Soc*. 2008; 14(1): 1–22; used with permission

that identify mTBI abnormalities that simply are not detected by CT imaging, this classification is mostly meaningless. Figure 10.3 demonstrated this point and another case is shown in Fig. 10.9. The presence of hemosiderin deposition is presumed to be the best marker for the existence of traumatic shear injury [31, 32].

Currently, the superior MRI method for detecting hemorrhagic shear lesions in mTBI is susceptibility weighted imaging (SWI).

CT imaging readily identifies more serious acute injuries or evolving TBI pathologies that require neurosurgical intervention and is of critical importance in the initial triage and medical management of TBI, including mTBI. With that being said, however, it is of limited utility in mTBI although some perfusion techniques as markers of initial neuroinflammation have shown an ability to detect mTBI abnormalities not identified on conventional DOI CT imaging [33, 34].

Visible Macroscopic Abnormalities

To best understand what information may be gathered from MRI in TBI, it is important to understand that the abnormalities are, in part, time dependent and differ by primary as well as secondary injury effects. Bigler and Maxwell [3, 4] have outlined a time frame depicting the potential pathological changes that occur as presented in the schematic shown in Fig. 10.10. Figure 10.11 shows how visibly detectable lesions change over time. Characteristic primary and secondary pathologies can be readily defined when sequential imaging is performed, typically a combination of CT and MRI, as shown in Fig. 10.11.

In Fig. 10.11 the acute CT findings depict the faint appearance of blood, mostly likely indicative of a traumatic subarachnoid hemorrhage. The presence of hemorrhage in TBI, whether detected by CT or MRI, is commonly considered the best indicator of intracranial traumatic shear forces sufficient to produce traumatic axonal injury (TAI) [3, 4]. However, even with the best of resolution that CT imaging provides precise detection and localization of the significance of this type of pathology is limited as demonstrated Fig. 10.11. By 8 days post-injury, edema is identified, but the hemorrhage has basically resolved where phagocytosis has removed degraded blood by-products. By 2 months post-injury, CT imaging demonstrates what appears to be resolution. However, when scanned 4 years later with MRI, hemosiderin deposition is distinctly apparent not in the subarachnoid space, but within brain parenchyma. Imaging of the gyri where the hemorrhage was identified also distinctly demonstrates signal abnormality beyond the hemosiderin foci. When viewed with MRI and knowing the sequence of events, the initial impact forces in this region likely sheared both blood vessels and neural tissue, resulting in DAI and focal WM changes. However, the DOI CT mostly depicts subarachnoid hemorrhage, with little indication of underlying WM damage. Only through sequential imaging does the true clinical significance of this injury become apparent.

From Fig. 10.11 the primary and secondary effects of TBI can be inferred. At the point of impact, the primary injury occurs and given the follow-up MRI findings there likely was traumatic shear injury resulting in primary axotomy. However, considerable secondary injury also likely occurred because of the edema as well as vascular injury and whatever local pathologic, metabolic, and neurotransmitter derangements and aberrations that occurred. Sheared blood vessels can no longer

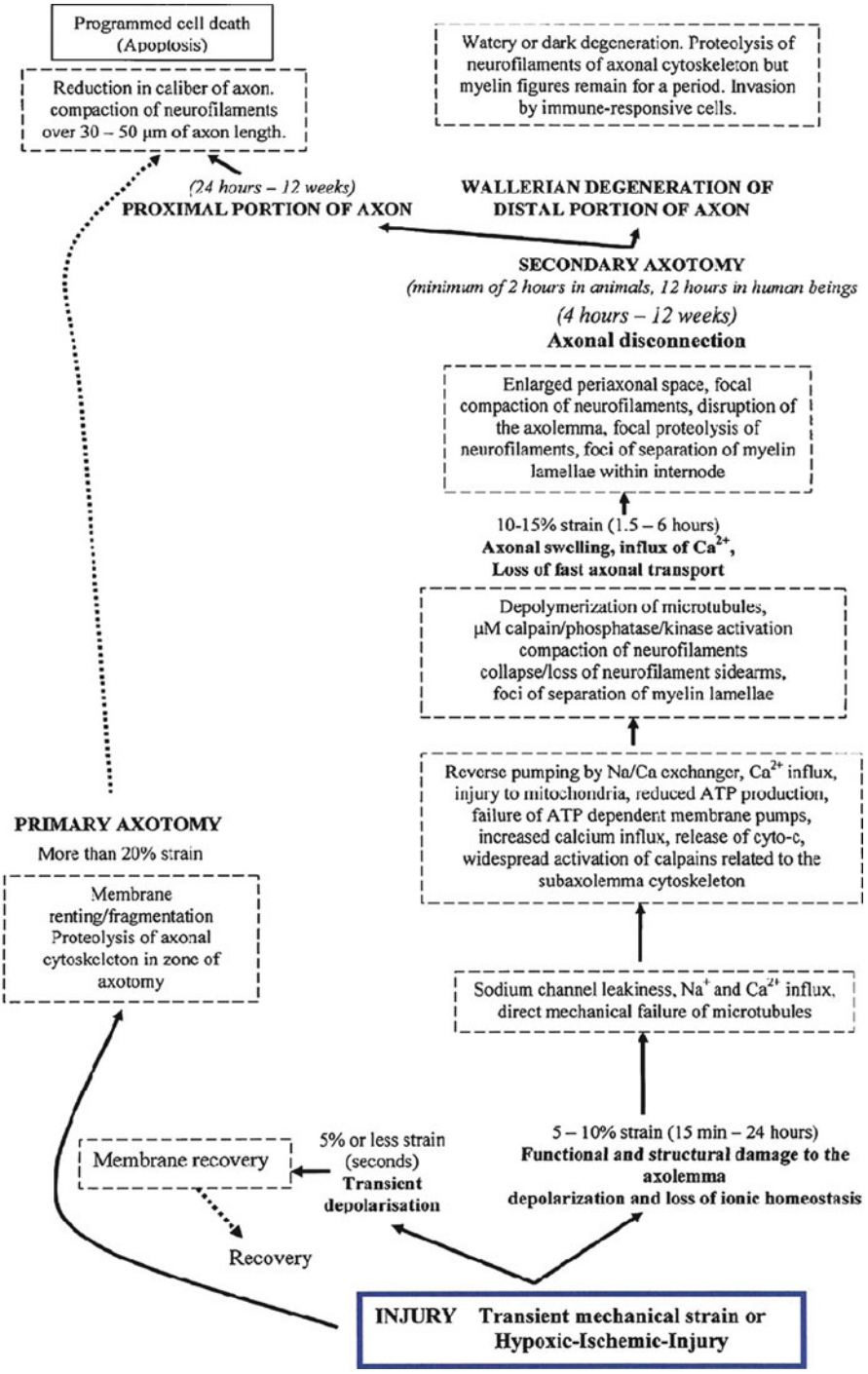

Fig. 10.10 Schematic overview of current thinking with regard to axonal injury in human DAI and animal diffuse traumatic brain injury. Modified from Biasca N, Maxwell WL. Minor traumatic brain injury in sports: a review in order to prevent neurological sequelae. Prog Brain Res 2007; 16: 263–291. From Bigler ED, Maxwell WL. Neuropathology of mild traumatic brain injury: relationship to neuroimaging findings—review. *Brain Imaging Behav*. 2012; 6(2): 108–136; used with permission

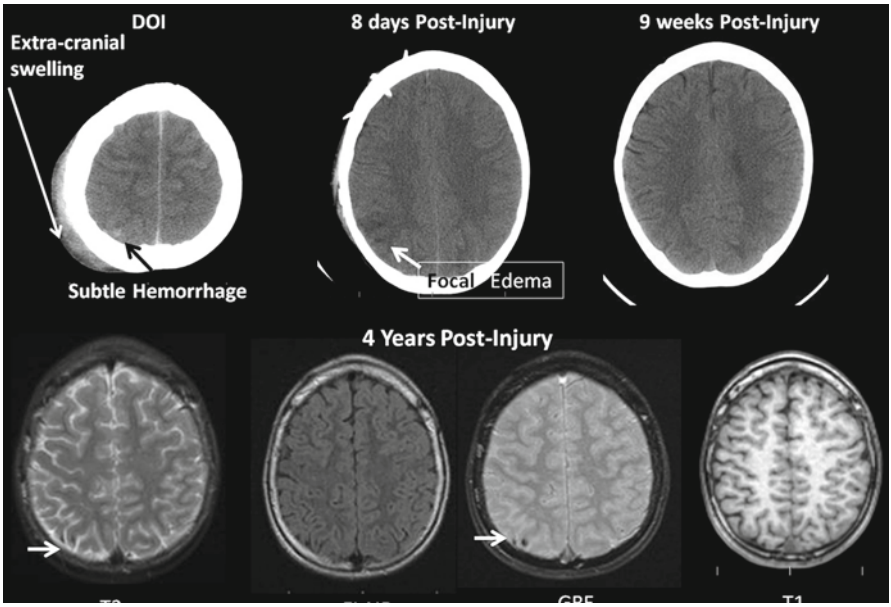

Fig. 10.11 Starting with the DOI CT scans, various lesion types are identified and using the DOI scan as baseline, changes from DOI to chronic state may be shown. The "lesion" starts off as a subtle subarachnoid hemorrhage but by 8 days post-injury is seen as edema which appears to resolve by 9 weeks post-injury. However, with follow-up MRI, subtle hemosiderin deposition is identified

provide oxygenated blood to the neuropil resulting in additional neural tissue (both neurons and glial cells) compromise, degradation, and potential death. Neuronal degeneration ensues which cannot be detected by CT imaging but is revealed by MRI. This potential sequence of events and its adverse influence on the axon is depicted in Fig. 10.12 [35].

Fig. 10.12 (continued) and local mitochondrial damage can follow, which, if unabated, collectively alters/impairs axonal transport illustrated in panel E. Alternatively, if these abnormalities do not progress, recovery is possible (F). When progressive, these events not only impair axonal transport but also lead to rapid intra-axonal change in the paranodal and perhaps internodal domains that elicit the collapse of the axolemma and its overlying myelin sheath to result in lobulated and disconnected axonal segments (G) that, over the next 15 min–2 h, fully detach (H). The proximal axonal segment in continuity with the cell body of origin now continues to swell from the delivery of vesicles and organelles via anterograde transport while the downstream fiber undergoes Wallerian change (I). Lastly, with the most severe forms of injury, the above identified calcium-mediated destructive cascades are further augmented by the poration of the axolemma, again primarily at the nodal region (J). The resulting calcium surge, together with potential local microtubular damage and disassembly, pose catastrophic intra-axonal change that converts anterograde to retrograde axonal transport, precluding continued axonal swelling, while the distal axonal segment fragments and disconnects (K), with Wallerian degeneration ensuing downstream (L). From Smith DH, Hicks R, Povlishock JT. Therapy development for diffuse axonal injury. *J Neurotrauma*. 2013; 30(5): 307–323; used with permission

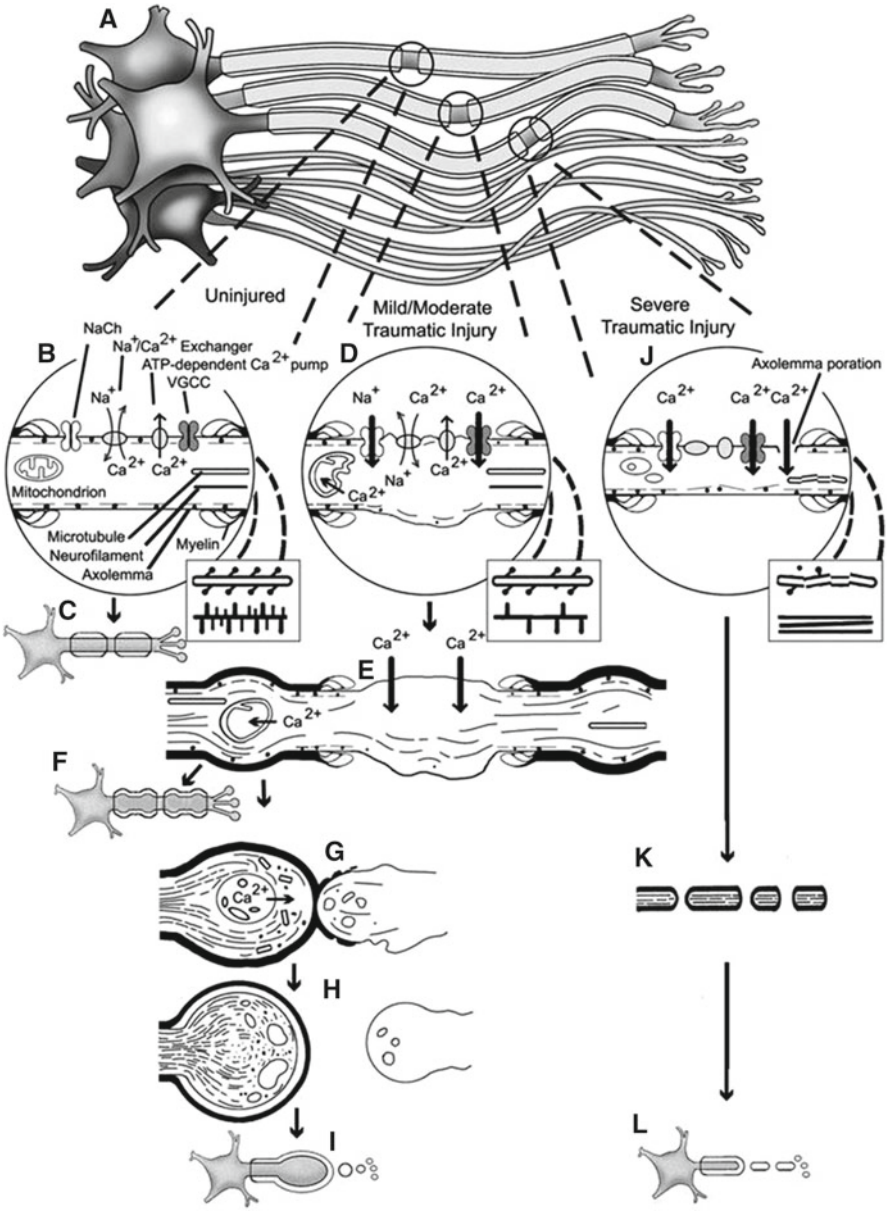

Fig. 10.12 Evolving pathophysiology of traumatic injury in myelinated axons. In this figure, the author's attempt, in an abbreviated fashion, to illustrate some of the key events believed to be involved in the pathobiology of traumatic axonal injury and, thereby, identify potential therapeutic targets. Although framed in the view of primary nodal involvement (A), this focus does not preclude comparable change ongoing in other regions of the axon. Panels B and C show normal axonal detail including the paranodal loops and the presence of intra-axonal mitochondria, microtubules, and neurofilaments, together with the presence of multiple axolemmal channels localized primarily to the nodal domain. Mild to moderate traumatic brain injury in panel D is observed to involve a mechanical dysregulation of the voltage-sensitive sodium channels, which contribute to increased calcium influx via reversal of the sodium calcium exchanger and the opening of voltage-gated calcium channels. This also impacts on the proteolysis of sodium channel inactivation that contributes further to local calcium dysregulation. Microtubular loss, neurofilament impaction,

Empirically Derived Quantitative MR Abnormalities

The common images generated from MR technology, like those shown in the various figures up to this point have all been generated by MR metrics that form the basis for the image display. However, these quantitative MR metrics permit analyses separate from just the anatomical image display. For example, Fig. 10.13 shows the appearance of a DTI MR sequence with its associated color map. Two common metrics derived from DTI are referred to as fractional anisotropy or FA and apparent diffusion coefficient or ADC. Figure 10.13 provides a DTI schematic depicting the relationship of FA and ADC to axon integrity and what happens with axon damage. These DTI metrics assess the microstructure of WM and are based on the characteristics of how myelin sheaths and cell membranes of WM tracts affect the movement of water molecules. Healthy axonal membranes constrain the free movement and direction of movement of water. Consequently, water molecules tend to move faster in parallel to nerve fibers rather than perpendicular to them. This characteristic, which is referred to as anisotropic diffusion and is measured by FA, is determined by the thickness of the myelin sheath and of the axons. FA ranges from 0 to 1, where 0 represents maximal isotropic diffusion (e.g., free diffusion in perfect sphere) and 1 represents maximal anisotropic diffusion, i.e., diffusion in one direction (e.g., a long cylinder of minimal diameter). Diffusion anisotropy varies across WM regions, putatively reflecting differences in fiber myelination, fiber diameter, and directionality.

The aggregate fiber tracts of an entire brain can be derived from DTI, as shown in Fig. 10.14. In TBI, DTI may demonstrate a loss of fiber tract integrity, reflected as a thinning out of the number of aggregate tracts. This is also demonstrated in

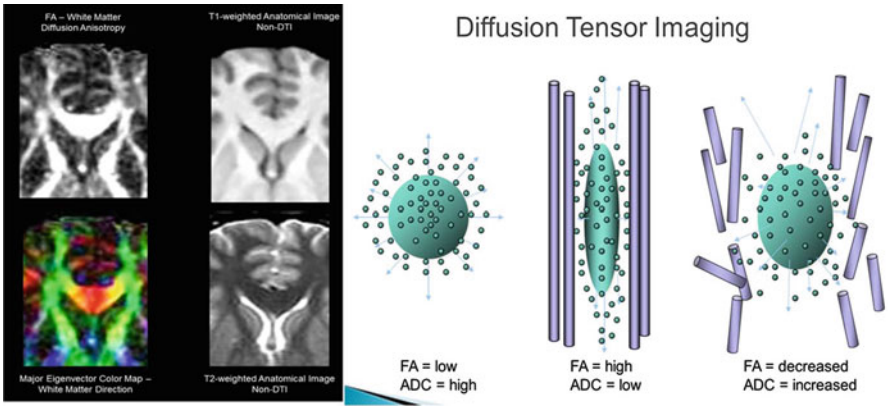

Fig. 10.13 The images on the *upper left* show the DTI acquisition image and the DTI color map (*bottom left*) in comparison to the conventional T1 and T2. The cartoon on the *right* depicts the relationship of fractional anisotropy (FA) with the apparent diffusion coefficient (ADC) showing how normal conformity of membrane anatomy constrains water diffusion; however, if membrane dissolution occurs in any fashion, such as from TBI, water is freer to move and with lack of constraint, FA elevates and ADC declines

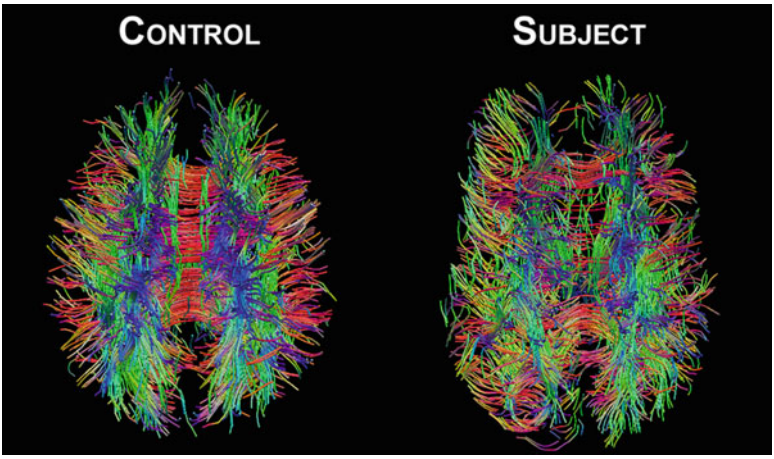

Fig. 10.14 The complexity of brain networks is readily appreciated in view whole brain DTI in a control subject and a patient with severe TBI showing reduced whole-brain network integrity. Note the WM thinning of aggregate tracts that has occurred in the case of TBI

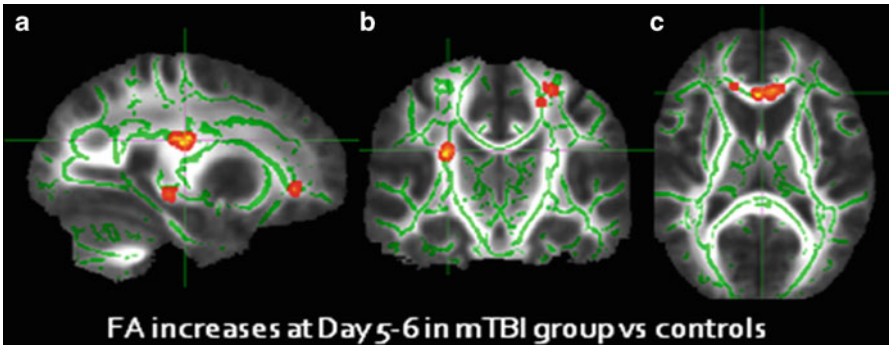

Fig. 10.15 In conjunction with the DTI demonstration of the fluctuation in fractional anisotropy (FA) and change in memory performance within the first 8 days post-injury (see Fig. 10.7), this tract-based spatial statistics output from this mTBI sample shows where there were significant regional increases in FA compared to controls. Possible interpretation of such findings is that they reflect areas of neuroinflammation. Interesting, it is at this point post-injury where some of the mTBI patients displayed their poorest performance on tasks involving memory function. (**a**) sagittal, (**b**) coronal and (**c**) axial MRI planes

Fig. 10.14, where a patient with TBI is compared to a similar aged individual with typical development. The loss of aggregate tracts in the TBI whole-brain network analysis demonstrates an overall reduction in WM connectivity. DTI methods provide various techniques to view the pathological effects of TBI within the context of WM network connectivity.

Figure 10.14 depicts the DTI findings in the individual case, but Fig. 10.15 provides an example of how group DTI findings may be presented. In this figure a

technique referred to as tract-based spatial statistics is used to show where significant group differences may be observed comparing the TBI group with a matched control sample. In Fig. 10.15, the mTBI patients first described in Fig. 10.7 were compared to matched controls with the results demonstrating distinctly visible differences in FA. In this illustration it shows where significant increases in FA were observed, interpreted to be an indication of neuroinflammation. Note the statistical comparison revealed abnormalities in the anterior and posterior corpus callosum, common regions for pathology to be detected when DTI is empirically assessed in mTBI.

Trauma-induced edematous reactions in the brain compress parenchyma, which in turn, may influence water diffusion potentially detected by DTI. Using the FA metric, increases in FA beyond some normal baseline may signify edema whereas low FA may occur when axon degradation, membrane abnormalities increase water diffusion or actual degeneration has occurred, which increases extracellular water. Since TBI may induce dynamic changes over time, differences in FA over acute, subacute, and chronic time frames post-injury may differ as well. When axons degenerate, the increased space frees extracellular water in resulting in lower FA. Thus, in mTBI, low FA may reflect WM degeneration.

Heterogeneity Visible MTBI Lesions

Bigler et al. [6] examined a sample of 41 children with complicated mTBI. When assessed with MRI at least 6 months post-injury regardless of whether the residual lesion was an area of focal encephalomalacia, hemosiderin deposit or WM hyperintensity, *none* of the lesions perfectly overlapped although the majority was distributed within the frontal and temporal lobes. Just from the randomness of the lesions, this would indicate that each mTBI produced its own unique injury and with unique injury this would indicate the likelihood that mTBI sequelae would likely be rather idiosyncratic to the individual as well.

Cellular Basis of MTBI Neuropathology

Based on the position statement by the International and Interagency Initiative toward Common Data Elements for Research on Traumatic Brain Injury and Psychological Health the definition of traumatic brain injury is "… an alteration in brain function, or other evidence of brain pathology, caused by an external force [36]". External force induces brain injury via deformation of neural tissue that surpasses tolerance limits for normal displacement or strain that accompanies movement such as jumping, rapid turning of the head, simple bumps to the head, etc. So, at the most fundamental level of injury, cellular deformation disrupts anatomy and physiology sufficient to at least transiently impair function when the threshold for mTBI has been reached.

Too often, neural cells are viewed schematically as an artist's rendition of what a neural cell looks like, such as that shown in Fig. 10.16 but artistic schematics detract

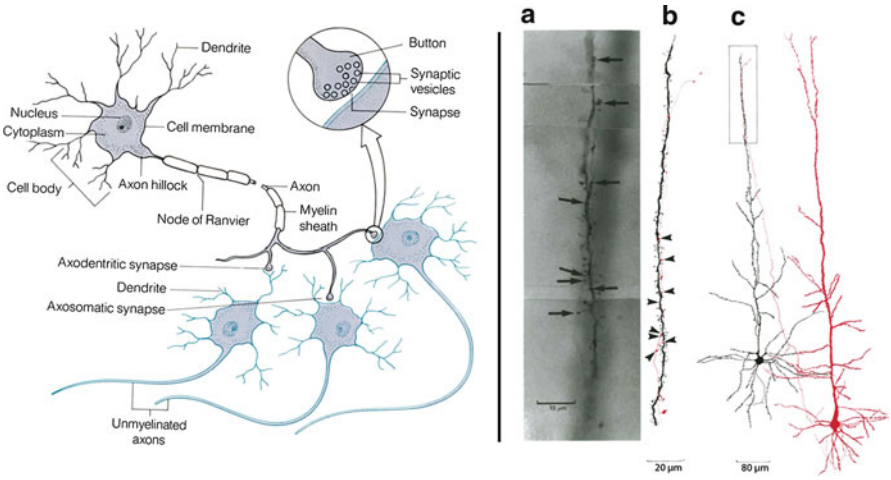

Fig. 10.16 (*Left*) The schematic of a neuron shows a hypothetical neuron with what appears to be a bulky, sturdy axon protruding from the cell body and interfacing with other neurons. However, the reality is something quite different. From: Pinel JPJ. Biopsychology. Boston: Allyn & Bacon, 1990; used with permission. (*Right*) Two cortical cells in a rat cortex that have been isolated. Note the micron level of the axon—it is infinitesimally small. Note also who the single axon intertwines the dendrite and the dendritic spines as highlighted in the photomicrograph. When thinking about TBI, one must view the potential neuropathological effects at this microscopic level. From Deuchars J, West DC, Thomson AM. Relationships between morphology and physiology of pyramid-pyramid single axon connections in rat neocortex in vitro. *J Physiol*. 1994; 478(3): 423–435; used with permission

from the true complexity and delicate nature of what really constitutes neural tissue. For example, Fig. 10.16 depicts two cortical pyramidal cells identified in the rat cerebral cortex, based on their physiological response and their appearance via electron microscopy. Note how small these structures are, note that these views are merely two-dimensional of a three-dimensional structure and note that the axon is but a few microns in thickness. Additionally note the numerous dendritic spines and how the axon intertwines with the spines.

As the definition implies, TBI occurs from some external force which, in turn must deform brain parenchyma such that a sufficient deformation of the typical shape of cellular tissue no longer lines up and/or connects as it should. Returning to Fig. 10.16, note again the complex intertwining of dendritic spines with axon segments where any misalignment would likely affect synaptic integrity. Likewise, if the axon membrane is disrupted, membrane permeability will directly impact neuronal function and propagation of axon potentials. Only one axon segment need be affected to disrupt neural transmission for the entire axon. A variety of finite elements and various methods for recreating the motion that displaces brain parenchyma that results in concussive injury have been performed, mostly using sports concussion models. For example, Viano et al. [37] showed on average in the typical sports-related concussion that the brain displaces between 4 and 8 mm in regions

like the corpus callosum, midbrain, medial temporal lobe, and fornix. Viewing Fig. 10.16 from the perspective of this amount of deformation, noting that the photomicrograph depicts an axon that is about 0.1 mm in length, would reflect a massive distortion of neurons this size.

Blood vessels are just as delicate as neural tissue, especially at the capillary level. Each neuron is dependent on receiving a continuous source of glucose and oxygen with the smallest capillaries largest enough for a just single red blood cell to traverse the capillary to deliver its oxygen and glucose [3, 4]. As such, blood vessels are just as susceptible to the shear–strain biomechanics of head injury as are neurons [38].

Deformation Biomechanics

From the above discussion all deformation in mTBI must be viewed at the cellular level, but biomechanical schematics are typically presented at the whole brain level. Ropper and Gorson [39] provided a schematic of where the greatest deformations have been modeled in mTBI and this is provided in Fig. 10.17. This illustration clearly depicts the known frontotemporal regions for cortical surface compression, but also WM tracts of the upper brainstem corpus callosum and cingulum. In mTBI, as already mentioned by definition of what constitutes a TBI the WM abnormalities at the brainstem level could not represent major pathology because LOC must be brief to meet mTBI criteria. Likewise, alteration in mental status that would result in prolong posttraumatic amnesia would also disqualify someone for mTBI classification. So while subtle brainstem pathology may persist in the mTBI patient, as Heitger et al. [40] have shown, as well as frontotemporal pathology, as numerous investigators have shown, major pathologies at these levels are unlikely because if major pathology persisted in these regions during the acute phase, the individual likely would not meet criteria for mTBI. Nonetheless, what is depicted in the Fig. 10.17 from Ropper and Gorson provides a wonderful heuristic for where likely changes in mTBI will be observed in neuroimaging studies.

For example, Fig. 10.18 is from a child with mTBI from a skiing accident who sustained an mTBI. When symptoms persisted, this child, who had a negative DOI CT was scanned with MRI. The follow-up MRI revealed hemosiderin deposition in frontotemporal areas and anterior corpus callosum, as would be predicted from the schematic in Fig. 10.17.

Volumetry Findings in MTBI

As shown in Fig. 10.17, if atrophic changes associated with mTBI were to occur, they would most likely be found within those regions associated with the greatest likelihood for shear/strain and deformation injury. Indeed, several studies that have prospectively examined mTBI subjects have demonstrated this regional atrophy [41–45].

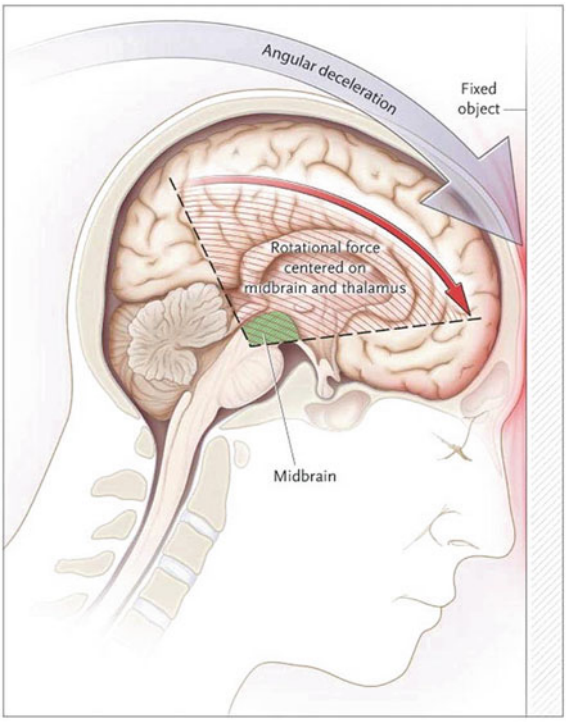

Fig. 10.17 The mechanism of concussion is outlined in this illustration. Biomechanical investigations dating back to the beginning of the twentieth century suggest that concussion results from a rotational motion of the cerebral hemispheres in the anterior–posterior plane, around the fulcrum of the fixed-in-place upper brain stem. If the neck is restrained, concussion is difficult to produce. Concussions as portrayed in movies and cartoons, in which the back of the head is struck with a blunt object and no motion is transferred to the brain, are implausible. The modern view is that there is disruption of the electrophysiological and subcellular activities of the neurons of the reticular activating system that are situated in the midbrain and diencephalic region, where the maximal rotational forces are exerted. Alternative mechanisms for concussive LOC, such as self-limited cortical seizures or a sudden increase in intracranial pressure, have also been proposed, but with limited supporting evidence. An animated version of this figure is available with the full text of the article at www.nejm.org. From Ropper AH, Gorson KC. Clinical practice. Concussion—review. *N Engl J Med*. 2007; 356(2): 166–172; used with permission

For example, Zhou et al. [42] demonstrated that by establishing a baseline in mTBI patients within the acute to early subacute time frame that when assessed with various volumetric techniques 1 year later that significant volume loss was observed in the anterior cingulum, cingulate gyrus, and scattered regions within the frontal lobes. Interestingly they observed volume loss in the cuneus and precuneus regions as well. The volume loss with the cuneus and precuneus, posterior brain regions may actually be the result of Wallerian degeneration from the more focal frontal loss disrupting long coursing frontoparietal connections particularly vulnerable to stretching and shearing effects [3, 4, 26].

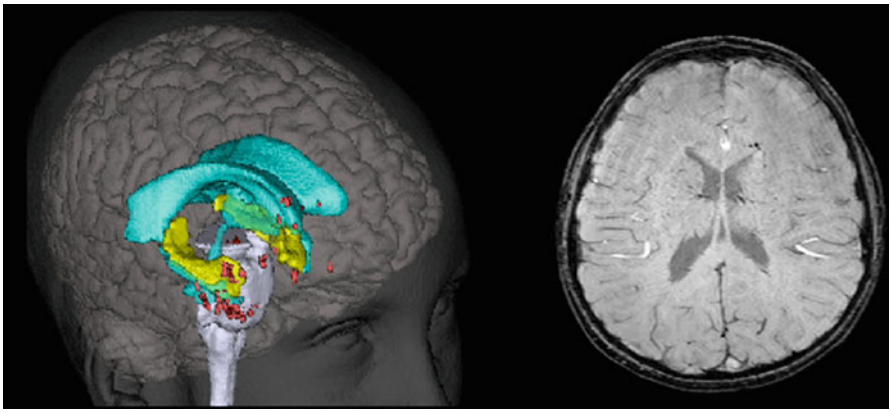

Fig. 10.18 This preadolescent child sustained an mTBI in a ski accident. When symptoms persisted MRI demonstrated multiple regions of hemosiderin deposition. Note the frontotemporal distribution and location of hemosiderin in the forceps minor region of the corpus callosum on the susceptibility weighted image on the *right*. In the three-dimensional image, the ventricle is shown in aquamarine to provide landmark points with the *red* signifying where hemosiderin was identified and the *yellow* indicates the hippocampus

Conclusion

Structural neuroimaging provides a variety of methods to detect underlying neuropathology that results from mTBI. The most common visible abnormalities are in the form of focal encephalomalacia, hemosiderin deposition, and/or WM hyperintensity. A variety of quantitative MRI methods have demonstrated techniques for the detection of underlying pathology associated with mTBI, which differ depending on the time post-injury that the scan is performed.

References

1. Yassa MA, Muftuler LT, Stark CE. Ultrahigh-resolution microstructural diffusion tensor imaging reveals perforant path degradation in aged humans in vivo. Proc Natl Acad Sci U S A. 2010;107(28):12687–91.
2. Heidemann RM, Ivanov D, Trampel R, Fasano F, Meyer H, Pfeuffer J, et al. Isotropic submillimeter fMRI in the human brain at 7 T: combining reduced field-of-view imaging and partially parallel acquisitions. Magn Reson Med. 2012;68(5):1506–16.
3. Bigler ED, Maxwell WL. Neuropathology of mild traumatic brain injury: relationship to neuroimaging findings—review. Brain Imaging Behav. 2012;6(2):108–36.
4. Bigler ED, Maxwell WL. Neuroimaging and neuropathology of TBI—review. NeuroRehabilitation. 2011;28(2):63–74.
5. Teasdale G, Jennett B. Assessment of coma and impaired consciousness. A practical scale. Lancet. 1974;2(7872):81–4.

6. Bigler ED, Abildskov TJ, Petrie J, Dennis M, Simic N, Taylor HG, et al. Heterogeneity of brain lesions in pediatric traumatic brain injury. Neuropsychology. 2013;27(4):438–51.
7. Dewitt DS, Perez-Polo R, Hulsebosch CE, Dash PK, Robertson CS. Challenges in the development of rodent models of mild traumatic brain injury. J Neurotrauma. 2013;30(9):688–701.
8. Hylin MJ, Orsi SA, Zhao J, Bockhorst K, Perez A, Moore AN, et al. Behavioral and histopathological alterations resulting from mild fluid percussion injury. J Neurotrauma. 2013;30(9): 702–15.
9. Jagoda AS. Mild traumatic brain injury: key decisions in acute management—review. Psychiatr Clin North Am. 2010;33(4):797–806.
10. Tavender EJ, Bosch M, Green S, O'Connor D, Pitt V, Phillips K, et al. Quality and consistency of guidelines for the management of mild traumatic brain injury in the emergency department. Acad Emerg Med. 2011;18(8):880–9.
11. Slobounov S, Gay M, Johnson B, Zhang K. Concussion in athletics: ongoing clinical and brain imaging research controversies—review. Brain Imaging Behav. 2012;6(2):224–43.
12. Wilde EA, Hunter BED. Pediatric traumatic brain injury: neuroimaging and neurorehabilitation outcome [Research Support, N.I.H., Extramural Review]. NeuroRehabilitation. 2012;31(3):245–60.
13. Wilde EA, Hunter JV, Bigler ED. A primer of neuroimaging analysis in neurorehabilitation outcome research—review. NeuroRehabilitation. 2012;31(3):227–42.
14. Wilde EA, Hunter JV, Bigler ED. Neuroimaging in neurorehabilitation. NeuroRehabilitation. 2012;31(3):223–6.
15. Post A, Hoshizaki B, Gilchrist MD. Finite element analysis of the effect of loading curve shape on brain injury predictors. J Biomech. 2012;45(4):679–83.
16. Statler KD, Swank S, Abildskov T, Bigler ED, White HS. Traumatic brain injury during development reduces minimal clonic seizure thresholds at maturity. Epilepsy Res. 2008;80(2–3): 163–70.
17. Bayly PV, Clayton EH, Genin GM. Quantitative imaging methods for the development and validation of brain biomechanics models [Research Support, N.I.H., Extramural Review]. Annu Rev Biomed Eng. 2012;14:369–96.
18. Feng Y, Okamoto RJ, Namani R, Genin GM, Bayly PV. Measurements of mechanical anisotropy in brain tissue and implications for transversely isotropic material models of white matter. J Mech Behav Biomed Mater. 2013;23C:117–32.
19. Kraft RH, McKee PJ, Dagro AM, Grafton ST. Combining the finite element method with structural connectome-based analysis for modeling neurotrauma: connectome neurotrauma mechanics. PLoS Comput Biol. 2012;8(8):e1002619.
20. Watanabe R, Katsuhara T, Miyazaki H, Kitagawa Y, Yasuki T. Research of the relationship of pedestrian injury to collision speed, car-type, impact location and pedestrian sizes using Human FE model (THUMS Version 4). Stapp Car Crash J. 2012;56:269–321.
21. Mao H, Elkin BS, Genthikatti VV, Morrison Iii B, Yang KH. Why is CA3 more vulnerable than CA1 in experimental models of controlled cortical impact-induced brain injury? J Neurotrauma. 2013;30(17):1521–30; Apr 4: epub ahead of print.
22. Feng Y, Clayton EH, Chang Y, Okamoto RJ, Bayly PV. Viscoelastic properties of the ferret brain measured in vivo at multiple frequencies by magnetic resonance elastography. J Biomech. 2013;46(5):863–70.
23. Prichep LS, McCrea M, Barr W, Powell M, Chabot RJ. Time course of clinical and electrophysiological recovery after sport-related concussion. J Head Trauma Rehabil. 2012;28(4):266–73; May 14: epub ahead of print.
24. Duhaime AC, Beckwith JG, Maerlender AC, McAllister TW, Crisco JJ, Duma SM, et al. Spectrum of acute clinical characteristics of diagnosed concussions in college athletes wearing instrumented helmets: clinical article. J Neurosurg. 2012;117(6):1092–9.
25. Stahel PF, Morganti-Kossmann MC, Kossmann T. The role of the complement system in traumatic brain injury—review. Brain Res Brain Res Rev. 1998;27(3):243–56.
26. Biasca N, Maxwell WL. Minor traumatic brain injury in sports: a review in order to prevent neurological sequelae—review. Prog Brain Res. 2007;161:263–91.

27. Magdesian MH, Sanchez FS, Lopez M, Thostrup P, Durisic N, Belkaid W, et al. Atomic force microscopy reveals important differences in axonal resistance to injury. Biophys J. 2012;103(3): 405–14.
28. Morrison B, Cater HL, Benham CD, Sundstrom LE. An in vitro model of traumatic brain injury utilising two-dimensional stretch of organotypic hippocampal slice cultures. J Neurosci Methods. 2006;150(2):192–201.
29. Wilde EA, McCauley SR, Barnes A, Wu TC, Chu Z, Hunter JV, et al. Serial measurement of memory and diffusion tensor imaging changes within the first week following uncomplicated mild traumatic brain injury. Brain Imaging Behav. 2012;6(2):319–28.
30. Wilde EA, McCauley SR, Hunter JV, Bigler ED, Chu Z, Wang ZJ, et al. Diffusion tensor imaging of acute mild traumatic brain injury in adolescents. Neurology. 2008;70(12):948–55.
31. Scheid R, Walther K, Guthke T, Preul C, von Cramon DY. Cognitive sequelae of diffuse axonal injury—a comparative study. Arch Neurol. 2006;63(3):418–24.
32. Scheid R, Preul C, Gruber O, Wiggins C, von Cramon DY. Diffuse axonal injury associated with chronic traumatic brain injury: evidence from T2*-weighted gradient-echo imaging at 3 T. AJNR Am J Neuroradiol. 2003;24(6):1049–56.
33. Metting Z, Rodiger LA, de Jong BM, Stewart RE, Kremer BP, van der Naalt J. Acute cerebral perfusion CT abnormalities associated with posttraumatic amnesia in mild head injury. J Neurotrauma. 2010;27(12):2183–9.
34. Metting Z, Rodiger LA, Stewart RE, Oudkerk M, De Keyser J, van der Naalt J. Perfusion computed tomography in the acute phase of mild head injury: regional dysfunction and prognostic value. Ann Neurol. 2009;66(6):809–16.
35. Smith DH, Hicks R, Povlishock JT. Therapy development for diffuse axonal injury. J Neurotrauma. 2013;30(5):307–23.
36. Menon DK, Schwab K, Wright DW, Maas AI. Position statement: definition of traumatic brain injury [Research Support, N.I.H., Extramural Research Support, Non-U.S. Gov't Research Support, U.S. Gov't, Non-P.H.S. Review]. Arch Phys Med Rehabil. 2010;91(11):1637–40.
37. Viano DC, Casson IR, Pellman EJ, Zhang L, King AI, Yang KH. Concussion in professional football: brain responses by finite element analysis: part 9—a comparative study. Neurosurgery. 2005;57(5):891–916.
38. Madri JA. Modeling the neurovascular niche: implications for recovery from CNS injury. J Physiol Pharmacol. 2009;60(4):95–104.
39. Ropper AH, Gorson KC. Clinical practice. Concussion—review. N Engl J Med. 2007;356(2): 166–72.
40. Heitger MH, Jones RD, Macleod AD, Snell DL, Frampton CM, Anderson TJ. Impaired eye movements in post-concussion syndrome indicate suboptimal brain function beyond the influence of depression, malingering or intellectual ability. Brain. 2009;132(10):2850–70.
41. Toth A, Kovacs N, Perlaki G, Orsi G, Aradi M, Komaromy H, et al. Multi-modal magnetic resonance imaging in the acute and sub-acute phase of mild traumatic brain injury: can we see the difference? J Neurotrauma. 2013;30(1):2–10.
42. Zhou Y, Kierans A, Kenul D, Ge Y, Rath J, Reaume J, et al. Mild traumatic brain injury: longitudinal regional brain volume changes. Radiology. 2013;267(3):880–90; Mar 12: epub ahead of print.
43. Ross DE, Castelvecchi C, Ochs AL. Brain MRI volumetry in a single patient with mild traumatic brain injury. Brain Inj. 2013;27(5):634–6.
44. Benson RR, Gattu R, Sewick B, Kou Z, Zakariah N, Cavanaugh JM, et al. Detection of hemorrhagic and axonal pathology in mild traumatic brain injury using advanced MRI: implications for neurorehabilitation. NeuroRehabilitation. 2012;31(3):261–79.
45. MacKenzie JD, Siddiqi F, Babb JS, Bagley LJ, Mannon LJ, Sinson GP, et al. Brain atrophy in mild or moderate traumatic brain injury: a longitudinal quantitative analysis. AJNR Am J Neuroradiol. 2002;23(9):1509–15.